Egypt. J. Chem. **Vol. 64,** No. 8 pp. 4653 - 4662 (2021)

Egyptian Journal of Chemistry

http://ejchem.journals.ekb.eg/

Beneficial Bioapplications of Silver Nanoparticles Synthesized by a Marine Crustacean *(Erugosquilla massavensis*)

D. M. Beltagy[a], N. I. Abdo[b]*, N. M. Samak[c], G. M. El-Khodary[c], K. K. Abdel-Aziz[c], M. H. Mona[d]

[a] *Biochemistry Division, Chemistry Department, Faculty of Science, Damanhour University, Damanhour, Egypt*
[b]*Department of Basic Sciences, Higher Institute of Engineering and Technology, New Borg El-Arab City, Alexandria, Egypt*
[c] *Zoology Department, Faculty of Science, Damanhour University, Damanhour, Egypt*
[d] *Zoology Department, Faculty of Science, Tanta University, Tanta, Egypt*

Abstract

Silver nanoparticles (AgNPs) have wide applications. Production of AgNPs can be occurred through different method chemical, physical, and green methods. The most popular methods are chemical approaches**.** Marine organisms exhibit a wide range of bioactivity. The present study was designed to establish the biosynthesis of silver nanoparticles from marine crustacean extract of the hard and soft parts of male and female *E. massavensis*. The microstructure, morphology and optical absorption properties of the nanoparticles were characterized by X-ray diffraction (XRD), scanning electron microscopy (SEM) and UV-visible spectroscopy. The formation of silver nanoparticles was confirmed by Uv-Vis absorption and the spectra were observed plasmon bands between 441.79–462.74 nm. XRD results show that the nanoparticles are crystalline in nature. SEM images detected the quasi-spherical AgNPs morphological shape. Silver nanoparticles from marine crustacean extract of the hard part of male *E. massavensis* (HM4) showed the best results in morphology and particle size. Evaluation of the cytotoxicity of AgNPs (HM4) on different cancer cell lines antiviral, anti-microbial, anti-diabetic, anti-arthritic, anti-aging and anti-inflammatory properties were assessed. AgNPs characterization may be introduced a promising applications in medical aspects.

Keywords: Silver nanoparticles; UV-Vis; SEM; XRD; Biosynthesis; Marine crustacean; Cytotoxicity; Bioapplications.

1. Introduction

Nanotechnology is a fast growing branch of science that deals with synthesis and development of varied nanomaterial. The field of nanotechnology is the most active area of research in modern materials science. Though there are many chemical as well as physical methods, green synthesis of nanomaterial is the most emerging method of synthesis [1-4]. Now, various kinds of metal nanomaterials are being prepared by copper, zinc, titanium, magnesium, gold, alginate and silver [5]. Silver nanoparticles AgNPs became the main focus of intensive research because of their wide selection of applications in areas like catalyst, optics, antimicrobials, and biomaterial production [6-8]. AgNPs have high reactivity due to the large surface to volume ratio and play a crucial role in inhibiting bacterial growth in aqueous and solid media. For instance, AgNPs have been reported to possess antitumor, antibacterial, antifungal, and antiviral activity [9].

Marine organisms are rich source of bioactive compounds with remarkable impact in the field of pharmaceutical, industrial and biotechnological product developments. Recent years, the researchers focusing research on synthesis of nanoparticles from marine sources [10]. Crustaceans, the major taxonomic group in marine ecosystems, occupy a large infaunal habitat and play an important role in bioturbation, transfer of organic materials and nutrients. Crustaceans are valued by the aquaculture industry as an excellent source of polyunsaturated fatty acids (PUFAs), and they have the potential to supplement fish oil as sources of essential lipid components of feeds [11]. The mantis shrimp

*Corresponding author e-mail: nabiha_ibrhim@yahoo.com.
Receive Date: 30 March 2021, Revise Date: 21 April 2021, Accept Date: 30 May 2021
DOI: 10.21608/EJCHEM.2021.70308.3549

(*Erugosquilla massavensis*) is an abundant crustacean in Egypt. It is common among the most important predators in many shallow, tropical and subtropical marine habitats. This mantis shrimp is found in high densities in areas with suitable burrowing substrates fine sand and sandy mud, especially where the influence of river run-off is important [12]. *E. massavensis* stomatopods are benthic, marine, predatory crustaceans that live in defendable burrows.

AgNPs have wide medical application one of the most important is anti-tumor effect against colorectal-cancer (CRC) which is the second leading cause of cancer mortality in many industrialized countries [13]. Colorectal cancer (CRC) accounts for 700,000 deaths and 1.4 million newly diagnosed cases globally per annum, making it the number one cause of non-smoking related cancer deaths. Cancers that start in the cells that line the inside of the colon and rectum are called colorectal cancers. Most CRCs arise in the epithelium, a process driven by genetic and/or epigenetic alterations that result in the formation of premalignant lesions called adenomas. Colorectal cancer (CRC) results from the progressive accumulation of genetic and epigenetic alterations that lead to the transformation of normal colonic epithelium to colon adenocarcinoma [14].

The present study was designed to establish the biosynthesis of silver nanoparticles from marine crustacean extract of the hard and soft parts of male and female *E. massavensis* and characterize silver nanoparticles that formed. The cytotoxicity of AgNPs that formed from the hard part of male *E. massavensis* was evaluated on different cancer cell lines. Antiviral, anti-microbial, anti-diabetic, anti-arthritic, anti-aging and anti-inflammatory properties were assessed.

Materials and Methods

Sample Collection

Mantis shrimp (*E. massavensis*) samples were obtained from Mediterranean Sea at Alexandria from Eastern Harbor. The samples were collected at night from (July to October) during summer of 2017 using commercial trawlers. The collected adult *E. massavensis* were brought to the laboratory in well-aerated seawater to ensure that they are still alive. Male (M) and female (F) mantis shrimp were easily separated according to thoracic genital regions and the presence or absence of penis. The morphometric analysis of male and female *E. massavensis* was determined by measuring the body length and body weight. Their weights were 17.80±3.79 g and 16.90±4.04 g, and lengths were 11.81±1.51and 11.78±1.28 cm for male and female, respectively. Separation of muscle away from exoskeleton by removing all appendages and the fresh whole bodies away from the carapace and stored at -20 °C until needed.

Preparation of extract

The muscles (soft part; S) and shell (hard part; H) (~10 g) was finely pulverized using mortar and pestle. The extract was made up to 100 mL using double-distilled Milli-Q water. Then the extract was filtered through Whatman number 1 filter paper to separate the tissue rubbles and obtain a pure extract.

Synthesis of silver nanoparticles

The filtrate was used as reducing agent and stabilizer for the synthesis of AgNPs. 10 mL of the filtrate was mixed with 90 mL of 1 mM silver nitrate solution in a 250 mL Erlenmeyer flask and agitated at 60 ^{o}C in dark. A flask containing 10 mL Milli-Q and 90 mL silver nitrate solution was taken as control. The change in colour was visually monitored till the appearance of typical dark brown colour.

Characterization of the synthesized silver nanoparticles (AgNPs)

The synthesized particles (SF1, HF2, SM3 and HM4) were characterized by absorption spectroscopy, SEM and XRD.

UV-Vis Spectroscopy

UV-visible spectroscopic analysis was carried out on Shimadzu UV 1700. After 24 hrs and 4 days, the optical density of synthesized nanoparticles suspended in distilled water was measured at different wavelength ranging from 300 to 800 nm and plotted the values on a graph.

X-Ray Diffraction Pattern

XRD measurements were recorded on (Shimadzu LabX XRD-6100 X-ray diffractometer, Japan). That was operated at a voltage of 40 kV and a current of 30 mA with an excitation source of CuKα radiation (λ= 1.541 Å), in the range of scanning angle 30 to 80^{o} at a scan rate of 5^{o}/min with the step width 0.02^{o}. For XRD measurements, the silver nanoparticles (AgNPs) were deposited on pre-washed glass substrates and dried in oven at 60 °C.

Scanning Electron Microscopy

The morphology of deposited AgNPs on glass substrates were analyzed using scanning electron microscopy (JEOL SEM, JSM-636OLA, Japan) at an accelerated voltage 20 kV. The samples surfaces were vacuum coated with gold for SEM.

Cytotoxicity evaluation

Different types of cell lines as MCF-7 (human breast cancer cell line), HepG-2 (human Hepatocellular carcinoma) and CACO (Colorectal carcinoma) were obtained from VACSERA Tissue

Culture Unit. The relation between surviving cells and drug concentration was continued for 24 h and viable cells yield was determined by a colorimetric method [15]. The 50% inhibitory concentration (IC50) was estimated from graphic plots of the dose response curve for each concentration.

Antimicrobial activity Assay

Cut plug method for screening of antimicrobial activity for tested complexes: recorded by **Pridham *et al*** [16] was employed to determine the antimicrobial activity of the chosen products. The average diameters of inhibition zones were recorded in millimetres, and compared for all plates. The antimicrobial profile was tested against Gram-positive bacterial species (*Staphylococcus aureus, Streptococcus mutants, Bacillus subtilis, Enterococcus faecalis, and Streptococcus pyogenes*), as well as Gram negative bacterial species (*Escherichia coli*, *Salmonella typhimurium*), and four fungi moulds (*Aspergillus fumigatus*, *Cryptococcus neoformas*, *Candida albicans*, and *Aspergillus Brasilienses*) using a modified well diffusion method.

Anti-viral effect

Evaluation of the antiviral activity using Cytopathic Effect Inhibition Assay on two viral strain HAV-10 (Hepatitis A virus) and HSV-1 (Herpes simplex type 1 virus), this assay was selected to show specific inhibition of a biologic function, i.e., cytopathic effect (CPE) in susceptible mammalian cells [17].

Anti-aging activity

Prior to screening in all assays, spectra for all extracts were recorded on a Cary 300 UV-visible spectrophotometer to check for interference and shifts in the lambda max. The assay employed was based on spectrophotometric methods by Collagenase assay [18] with some modifications for use in a microplate reader.

Anti-inflammatory and Anti-arthritic activities

Anti-inflammatory properties of both crude extract and synthesized silver nanoparticles were evaluated using albumin denaturation test with some modifications [19]. While, Anti-arthritic activities were assessed using U937 human monocytes (ATCC, Manassas, VA, USA) to study the effect of samples on histamine release [20].

Evaluation of Anti-diabetic Potential

Antidiabetic activities for both the crude extract and the synthesized silver nanoparticles were evaluated by two different methods. The first was α-glucosidase inhibitory activity which was measured according to the method described by **You *et al.*** [21]. The second was, α-amylase inhibitory activity that was determined by a colorimetric microplate assay utilizing a well-established protocol [22].

Statistical analysis

Data were expressed as mean values ± SD (standard deviation) and statistical analysis was performed using one-way analysis of variance (ANOVA) to assess significant differences among treatment groups. The criterion for statistical significance was set at $p \leq 0.05$. All statistical analyses were performed using SPSS statistical version 17 software package (SPSS® Inc., USA).

Results and Discussion

It has been successfully carried out the synthesis of silver nanoparticles by chemical reduction method. The formation of silver nanoparticles was observed visually with discoloration (brown) after incubation. Brown color is formed on the sample indicates that the colloidal nanoparticles produced are the synthesis process is dominated by grains of silver nanoparticles.

UV-visible spectroscopy

Ultraviolet and visible spectrometry is almost used for quantitative analysis of compound known to be present in the sample. UV-visible spectroscopy is one of the most widely used techniques for structural characterization of silver nanoparticles.

In metal nanoparticles such as in silver, the conduction band and valence band lie very close to each other in which electrons move freely. These free electrons give rise to a surface plasmon resonance (SPR) absorption band [23-26], occurring due to the collective oscillation of electrons of silver nanoparticles in resonance with the light wave [27].

Optical absorption spectra of silver nanoparticles is dominated by SPR which shows a shift towards the red end or blue end depends on particle size, shape, state of aggregation of the resulting silver nanoparticles [28].

The absorption spectra of the samples (SF1, HF2, SM3 and HM4) show a well-defined plasmon bands between 441.79–462.74 nm after 24 hrs, which are characteristic of nanosized silver. The UV-Vis absorption spectra of the AgNPs samples (SF1, HF2, SM3 and HM4) are displayed in **Figure 1**.

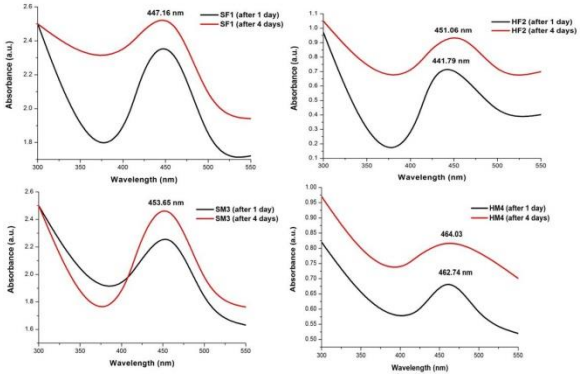

Figure 1. UV-Vis absorption spectra of colloidal silver nanoparticles synthesized (SF1, HF2, SM3 and HM4).

Silver nanoparticles samples (SF1 and HM2) showed the appearance in the electronic absorption spectra of bands located at 447.16 nm and 441.79 nm after 24 hrs (1 day), respectively associated with the presence of some irregular shapes. While Absorption bands of SM3 and HM4 samples appear at longer wavelengths associated with small roughly spherical and spherical nanoparticles.

The reaction mixture showed a surface plasmon resonance absorption band with a maximum peak of 462.74 nm and 453.65 nm after 24 hrs, respectively indicating the presence of spherical or roughly spherical shape silver nanoparticles. Broadening of peak indicated that the particles are polydispersed [29, 30].

The stability of synthesized silver nanoparticle solutions was assessed by recording the UV-vis spectra at intervals of 1 and 4 days. There was no obvious change in peak position of silver nanoparticles (SF1, SM3 and HM4), except for the increase of absorbance. Increase of absorption indicates that amount of silver nanoparticles increases. The stable position of absorbance peak indicates that new particles do not aggregate. As for the sample HF2, the position of the peak has a slight red shift (451.06 nm), implying the onset of nanoparticle aggregation.

SEM analysis

Silver nanoparticles were subjected to SEM micrograph analysis to understand the topology of silver ions. The silver nanoparticles morphology was studied by means of scanning electron microscopy (SEM). SEM micrographs of SF1, HF2, SM3 and HM4 nanoparticles being synthesized are displayed in **Figure 2**.

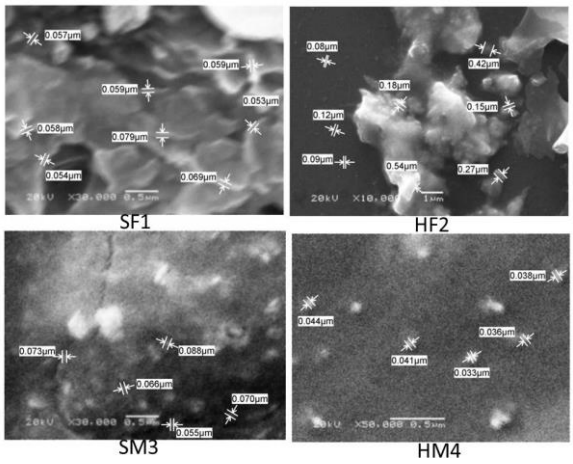

Figure 2. SEM Micrographs of silver nanoparticles (SF1, HF2, SM3 and HM4)

According to SEM analysis the silver nanoparticles were spherical (in case of HM4), roughly spherical (in case of SM3), plate and some irregular (in case of SF1 and HF2).

XRD Analysis

The structure of prepared silver nanoparticles has bee n investigated by X-ray diffraction (XRD) analysis. XRD of SF1, HF2, SM3 and HM4 nanoparticles are displayed in **Figure 3**.

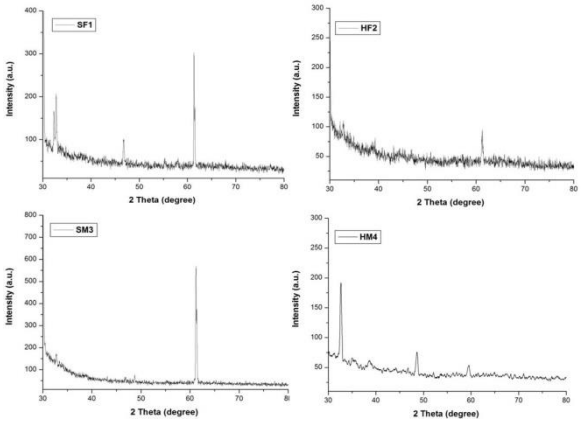

Figure 3. XRD patterns of silver nanoparticle (SF1, HF2, SM3 and HM4)

The average particle size has been estimated by using Debye-Scherrer formula [27, 31].

$$[D = 0.9\ \lambda/\beta\ \cos\Theta]$$

Where 'λ' is wave length of X-Ray (0.1541 nm), 'β' is FWHM (full width at half maximum),
'θ' is the diffraction angle and 'D' is particle diameter (size).

The X-ray diffraction pattern of the synthesized nanoparticles (SF1) shows diffraction peaks at 2θ = 32.31º, 32.77º, 46.70º and 61.34º, which can be

respectively indexed to (111), (111), (210) and (310) lattice planes.

The X-ray diffraction pattern of the synthesized nanoparticles (HF2) shows diffraction peaks at 2θ = 32.10º, 39.28º and 61.24º, which can be respectively indexed to (111), (200) and (310) lattice planes.

The X-ray diffraction pattern of the synthesized nanoparticles (SM3) shows diffraction peaks at 2θ = 32.72º, 48.68º and 61.20º, which can be respectively indexed to (111), (211) and (310) lattice planes.

The X-ray diffraction pattern of the synthesized nanoparticles (HM4) shows diffraction peaks at 2θ = 32.62º, 48.58º and 59.46º, which can be respectively indexed to (111), (211) and (300) lattice planes.

The high intensity peaks for silver nanoparticles in samples (SF1, HF2 and SM3) were observed at 2θ = 61.34º, 61.24º, 61.20º, respectively are corresponding to (310) reflection. This confirmed the lattice structures to be bcc (body centered cubic).

A number of Bragg reflections in the (111), (211) and (300) set of lattice planes were observed for silver nanoparticles sample (HM4). The high intensity for fcc materials is generally (111) reflection, which is observed in the sample from the most intense peak at 2θ = 32.62º. This confirmed the lattice structure to be fcc (face centered cubic). Silver nanoparticles samples (SF1, HF2) and (SM3, HM4) data are presented in **Table 1 (a, b)**, respectively.

It has been found that the coexistence of bcc (SF1, HF2 and SM3) and fcc (HM4) crystal structures appears with the change of reducing agents (soft and hard parts of organism).

Lattice constant has been estimated using the formula, $a = d*\sqrt{(h^2+k^2+l^2)}$ for silver nanoparticles samples (SF1, HF2, SM3 and HM4). Average of the four values of 'a' calculated from the values of 'd' as obtained from the data for the peaks is found to be 4.66, 4.73, 4.69 and 4.66 Å, respectively. It is observed that the lattice parameters of silver nanoparticles decrease with decreasing of the particle size.

Average size of the nanoparticles particles samples (SF1, HF2, SM3 and HM4) was found to be 67.07, 557.03, 80.66 and 20.63 nm, respectively. In the case of particles synthesized in HM4 media the mean particle size was 20.63 nm while particles synthesized in SF1, HF2 and SM3 were larger on an average. The XRD results show that the nanoparticles are crystalline in nature and the crystals are cubical in shape.

HF2 was found to have unusually large size. The larger silver particles were clustered may be due to the aggregation of the smaller ones.

The analysis of XRD patterns confirmed the results obtained from UV-Vis spectra and electron micrographs of the synthesized nanoparticles.

Bioapplications

Owing to the observed characterization of the biosynthesis of silver nanoparticles from marine crustacean extract of the hard and soft parts of male and female *E. massavensis* (SF1, HF2, SM3 and HM4), exploiting the best results of AgNPs (HM4) for evaluation of the cytotoxicity on different cancer cell lines antiviral, anti-microbial, anti-diabetic, anti-arthritic, anti-aging and anti-inflammatory properties.

Table 1. XRD results of synthesized silver nanoparticles:

(a) SF1 and HF2

Diffraction angle [2Θ] (degree)	FWHM [β] (radian)	Size [D] (nm)	d_{hkl}-spacing (Å)	Diffraction planes (hkl)	Relative intensity (%)
[32.31] 16.15	0.0018	80.22	2.76	111	31.66
[32.77] 16.38	0.0028	51.63	2.73	111	40.15
[46.70] 21.85	0.0029	51.53	1.94	210	21.23
[61.34] 30.67	0.0019	84.90	1.51	310	100
Average particle size [D] of **SF1**= 67.07 nm					
Lattice constant [a] of SF1= 4.66 Å					
[32.10] 16.05	0.0001	1443.20	2.78	111	67.5
[39.28] 19.64	0.0010	147.30	2.29	200	65
[61.24] 30.62	0.0016	80.60	1.51	310	100
Average particle size [D] of **HF2**= 557.03 nm					
Lattice constant [a] of HF2= 4.73 Å					

(b) SM3 and HM4

Diffraction angle [2Θ] (degree)	FWHM [β] (radian)	Size [D] (nm)	d_{hkl}-spacing (Å)	Diffraction planes (hkl)	Relative intensity (%)
[32.72] 16.36	0.0016	90.30	2.73	111	8.19
[48.68] 24.34	0.0018	84.60	1.86	211	5.65
[61.20] 30.60	0.0024	67.10	1.51	310	100
Average particle size [D] of **SM3**= 80.66 nm					
Lattice constant [a] of SM3 = 4.69 Å					
[32.62] 16.31	0.0066	21.90	2.74	111	100
[48.58] 24.29	0.0076	20.02	1.87	211	34.48
[59.46] 29.73	0.0080	19.98	1.55	300	13.79
Average particle size [D] of **HM4** = 20.63 nm					
Lattice constant [a] of HM4 = 4.66 Å					

The results obtained from the cytotoxicity test against different cell lines for both crude extract and AgNPs of hard part of male *E. massavensis* **(Table 2)** indicated that, AgNPs that synthesized from hard part of male *E. massavensis* have relatively strong cytotoxic properties against all the tested cell lines (derived from colon, breast, and liver cancer) than the crud extract from hard part male *E. massavensis.*

IC50 values of the cytotoxicity obtained by AgNPs were nearly close to those obtained by the reference drug especially in colon cancer. These results are in line with different previous studies which were proved that AgNPs synthesized from honey bee extract showed high relative activity against CACO cell line derived from human colon cancer with 58.6 % inhibition [32, 33]. Other study indicated that AgNPs were able to reduce viability of Dalton's lymphoma ascites tumor [34]. AgNPs from common medicinal plants as *Taraxacum officinale* and *Commelina nudiflora* showed their high cytotoxic effect against human liver cancer cells (HepG2) and colon cancer cells (HCT-116) [35, 36]. It can be explained by the fact that inside cells, nanoparticles easily cross the nuclear membrane and profoundly interact with intracellular macromolecules like proteins and DNA. Biologically synthesized AgNPs capable to alternation cell morphology of cancer cells which an early indicator for apoptosis which can be determined by structural alternation in cells [37].

The data were obtained from the antimicrobial assessment of both crude and AgNPs from shell of *E. massivansis* **(Table 3)** indicated better anti-bacterial activity against Gram-positive bacteria (*Staphylococcus aureus*, *Streptococcus mutants*, *Bacillus subtilis*, *Enterococcus faecalis*, and *Streptococcus pyogenes*) by inhibition zones ranged from 9-15 mm diameter. While, the crude extract showed no activity. On the other hand, AgNPs showed good anti-bacterial activity against Gram-negative bacteria (*Salmonella typhimurium, Pseudomonas aeruginosa, Escherichia coli, and Klebsiella pneumonia*) with inhibition zones ranged from 10-14 mm diameter. The crude extract from shell of male *E. massivansis* showed similar results with inhibition zones ranged from 10-16 mm diameter except against *E. coli* which did not show any activity. By a similar manner with Gram-positive bacteria, AgNPs also showed relatively medium anti-fungal activity against *Aspergillus fumigatus, Cryptococcus neoformas, Candida albicans, and Aspergillus Brasilienses* with inhibition zones of 10-15 mm diameter. However, crude extract show no activity. These results are in the line with other previous studies reported that AgNPs from haemolymph of marine crabs (*Carcinus maenas*, *Ocypode quadrata* and polychaeta) showed high antibacterial activity against different pathogens.

It can be discussed according to their large activity surface area of AgNPs which enable them to achieve better contact with microorganism. Nanoparticles get adsorb on to the cell membrane and enter inside bacterial cells which interact with sulfur containing protein in cell membrane of bacteria as well as phosphorus continuing compound like DNA. The AgNPs cause inhibition of replication of DNA of bacterial cell that causes inhibit cell division which cause bacterial cell death [38, 39]. Other important application of AgNPs is antiviral activity.

Table 2. IC50 of the crude extract and AgNPs (HM4) synthesized from hard part of male *E. massavansis* against CACO (*Colorectal*), MCF-7 (breast) and HepG-2 (liver) cell lines.

Extract	IC50 (µg/ml)		
	Colon	Breast	Liver
Crude extract of hard part of *E. massavansis*	229±1.89	>1000±3.50	416±2.78
AgNPs (HM4) synthesized from hard part of *E. massavansis*	3.73±0.67	10.7±2.44	13.1±1.34
Reference drug (*Doxorubicin*)	1.93±0.34	0.35±0.09	0.36±0.07

Table 3. Anti-microbial activity of crude extract and AgNPs (HM4) synthesized from hard part of male *E. massavansis*.

Extract	Inhibition zone (mm)					
	Gram-positive bacteria					
	S. aureus	*S. mutants*	*B. Subtilis*	*E. Faecalis*	*S. Pyogenes*	Reference drug (*Gentamycin*)
AgNPs (HM4)	10	15	10	11	9	17
Crude	0	0	0	0	0	
Gram-negative bacteria						
	S. typhimurium	*P. Aeruginosa*	*E. coli*	*K. pneumonia*		Reference drug (*Gentamycin*)
AgNPs (HM4)	11	14	10	11		17
Crude	9	10	0	16		
Fungi						
	A. fumigatus	*C. neoformas*	*C. albicans*	*A. Brasilienses*		Reference drug (*Ketoconazole*)
AgNPs (HM4)	10	15	10	11		17
Crude	0	0	0	0		

The results obtained in our study reported that antiviral activity of AgNPs that synthesized from exoskeleton of male *E. massavensis* showed moderate antiviral effect against HAV-10 and weak effect against HSV-1 **(Table 4)**. On the other hand, crude extract from hard part of male *E. massavensis* showed no antiviral activity. these results are in agreement with previous study indicated that the effect of AgNPs on many types of virus infection as human Immunodeficiency Virus Type 1 (HIV), Herpes Simplex Virus Type 1 HSV-1, Hepatitis B Virus (HBV), Monkey pox Virus, Tacaribe virus (TCRV), and Respiratory syncytial virus [40]. AgNPs that synthesized from shell of male *E. massavensis* also showed a relatively higher anti-aging activity than crude extract. These results are in the same line with many previous studies demonstrated that role of AgNPs in protection against UVB induced photoaging and the role of nanoparticles in Cosmeceuticals used for skin, hair, nail, and lip care [41, 42].

AgNPs that synthesized from exoskeleton of male *E. massavensis* showed moderate anti-Arthritic activity using of inhibition of protein denaturation method. While, crude extract has very low anti-Arthritic activity as comparing with *Diclofenac sodium* as standard compound **(Table 5)**. These results are in agreement with previous study reported that AgNPs from marine invertebrates could be used as potent anti-arthritic agent due to containing bioactive compounds which used for preventing inflammation with its associated pain and reduced mobility symptoms is a primary requirement in arthritis treatment [43, 44]. It has been reported that one of the features of several non-steroidal anti-inflammatory drugs is their ability to stabilize and prevent denaturation [45].

In this study, AgNPs (HM4) that synthesized from hard part of male *E. massavensis* have higher anti-diabetic potential of α-*glucosidase* and α-*amylase* inhibitory activity than crude extract as compared with *Acarbose* as standard compound **(Table 5)**.

These results are in agreement with different previous studies reported that the significant reduction in blood sugar in rat treated with AgNPs using *P. sapota* and *Lonicera japonica* leaf extract and demonstrated that AgNPs exhibit anti-diabetic activity, as evaluated *in vitro* and *in vivo*. SNPs were elucidated as antidiabetic agents that lead to reduction of blood glucose [46-48].

Table 4. Anti-viral and anti-aging activities of crude extract and AgNPs synthesized from hard part of male *E. massavansis*.

Extract	Anti-viral effect		Anti-aging Effect (IC50 µg/ml)
	HSV-1 Herpes Simplex type 1 Virus	HAV-10 Hepatitis A Virus	
Crude	-ve	-ve	229.5±3.68
AgNPs (HM4)	Weak antiviral effect	Moderate antiviral effect	37.60±1.12

Table 5. Anti-diabetic, anti-arthritic and anti-inflammatory activities of crude extract and AgNPs synthesized from hard part of male *E. massavansis*.

Extract	Anti-Diabetic (IC50 µg/ml)		Anti-arthritic (IC50 µg/ml)	Anti-inflammatory (IC50 µg/ml)
	α-amylase inhibitory	*α-glucosidase* inhibitory		
Crude	200.37±2.78	145.47±2.07	915.34±4.35	192.13±3.40
AgNPs (HM4)	120.78±1.99	66.80±1.34	118.47±1.88	29.70±1.50
Reference drug	*Acarbose* 34.71±1.07	*Acarbose* 30.57±0.62	*Diclofenac sodium* 15.12±0.83	------

Conclusions

Silver nanoparticles synthesized by chemical reduction method by using marine crustacean extract of the hard and soft parts of male and female *E. massavensis*. The nanoparticles were characterized by UV-Vis spectroscopy, SEM and XRD. The analysis of XRD patterns confirmed the results obtained from UV-Vis spectra and electron micrographs of the synthesized nanoparticles. AgNPs (HM4) exhibited cytotoxic action on different cancer cell lines antiviral, anti-microbial, anti-diabetic, anti-arthritic, anti-aging, and anti-inflammatory. AgNPs characterization may be introduced a promising applications in medical aspects.

Conflicts of interest

There are no conflicts to declare

References

1. Umayaparvathi, S., Arumugam, M., Meenakshi, S. and Balasubramanian, T., Biosynthesis of Silver Nanoparticles using *Oystersaccostrea Cucullata* (born, 1778): Study of in-vitro antimicrobial activity. *Int. J. Sci. Nat*., 4(1) 199-203 (2013).

2. Abdel-Raouf, N., Al-Enazi, N.M., Ibraheem, I.B.M., Alharbi, R.M. and Alkhulaifi, M.M.,
Biosynthesis of Siver Nanoparticles by using of the Marine Brown Alga Padina Pavonia and their Charactrrization. *Saudi Journal of Bilogical Sciences*, 26, 1207-1215 (2019).

3. Xu, L., Wang, Y., Huangg, J., Chen, C., Wang, Z. and Xie, H., Silver Nanoparticles: Synthesis, Medcal Applications and Biosafety. Theranostics, 10(20), 8996-90—31 (2020).

4. Dawadi, S., Katuwal, S., Gupta, A., lamichhane, U., Thpa, R., Jaisi, S.., Lamichhane, G., Bhattarai, D.P. and Parajuli, N., Current Research on Silver Nanoparticles: Synthesis, Characterization, and Applcations. *Journal of Nanomaterials*, 2021, 1-23 (2021).

5. Basavaraj, U., Praveenkumar, N., Sabiha, T.S., Rupali, S., and Samprita, B., Synthesis and characterization of silver nanoparticles. *Int. J. Pharm. Bio Sci*., 3, 10-14, (2012).

6. Qin, X. , Lu, W., Luo, Y., Chang, G., and Sun, X. Preparation of Ag nanoparticle-decorated polypyrrole colloids and their application for H2O2 detection Electrochem. *Commun*., 13 (8): 785-787 (2011).

7. Bhuyar, P., Rahim, M.H.A., Sundararaju, S., Ramaraj, R., Maniam, G.P. and Govindan, N., Syntesis of Silver Nanoparicles using marine Macroalagae Padina sp. And its antibacteria Activity towards Pathogenic Bacteria. *Beni-Suef University Journal of Basic and Applied Sciences*, 9(3), 1-15 (2020).

8. Almatroudi, A., Silver Nanoparrtcles: Synthesis, Characteization and Biomedical Applicaions. *Open Life Sciences*, 15, 819-839 (2020).

9. Zhang, Y., Wang, L., Tian, J., Li, H., Luo, Y. and Sun, X., Ag poly(m-phenylenediamine) Core–shell

Nanoparticles for Highly Selective, Multiplex Nucleic Acid Detection. *Langmuir*, 27, 2170-2175 (2011).

10. Asmathunisha, N. and Kathiresan, K., A review on Biosynthesis of Nanoparticles by Marine Organisms. *Colloids Surf. B.*, 103, 283–287, (2013).

11. Stabili, L., Sicuro, B. and Dapr`a, F., The Biochemistry of *Sabella spallanzanii* (Annelida: Polychaeta): A potential Resource for the Fish Feed Industry. *J. World Aquacult. Soc*., 44(3), 384–395 (2013).

12. Atkinson, R.J.A., Froglia, C., Arneri, E. and Antolini, B., Observation on the Burrows and Burrowing Behaviour of *Squilla mantis (L.)* (Crustacea: Stomatopoda). *Mar. Ecol*., 18(4), 337-359 (1997).

13. Jemal, A., Siegel, R., Ward, E., Murray, T. and Xu, J., Cancer statistics. *CA Cancer J. Clin*., 56(2), 106–130 (2006).

14. Elrasheid, A., Kheirelseid, H., Miller, N. and Kerin, M.J., Molecular Biology of Colorectal Cancer: Review of the Literature. *Am. J. Mol. Biol*., 3, 72-80, (2013).

15. Mosmann, T., Rapid Colorimetric Assay for Cellular Growth and Survival: Application to Proliferation and Cytotoxicity Assays. *J. Immunol. Methods*, 65(1-2), 55-63 (1983).

16. Pridham, T., Lindenfelser, L., Shotwell, O., Stodola, F., Benedict, R., Foley, C., Jacks, P., Zaumeyer, W., Perston, W. and Mitchell, J., Antibiotics against Plant Diseases: A laboratory and Green House Survey. *Phytopathology*, 46, 568-575 (1956).

17. Hu, J.M. and Hsiung, G.D., Evaluation of New Antiviral Agents I: In vitro Prospectives. *Antiviral Res.*, 11(5-6), 217-232 (1989).

18. Van Wart, H.E. and Steinbrink, D.R., A continuous Spectrophotometric Assay for Clostridium histolyticum Collagenase. *Anal. Biochem*., 113(2), 356-365 (1981).

19. Singh, S. and Sharma, N., Evaluation of In vitro Anti-arthritic Activity of Acacia auriculiformis a. Cunn. Ex. Benth. Stem bark. *World J. Pharm. Pharm. Sci.*, 5(2), 1659-1664 (2016).

20. Venkata, M., Sripathy, R., Anjana, D., Somashekara, N., In Silico, In Vitro and In Vivo Assessment of Safety and Anti-inflammatory Activity of Curcum. *American Journal of Infectious Diseases*, 8(1): 26-33 (2012).

21. You, Q., Chen, F., Wang, X., Luo, P. G. and Jiang, Y., Inhibitory Effects of Muscadine anthocyanins on Alpha-glucosidase and Pancreatic Lipase Activities. *J. Agric. Food Chem*., 59(17), 9506-9511 (2011).

22. Ingrid, F. and Matthias, F.M., Traditionally used Plants in Diabetes Therapy: Phytotherapeutics as Inhibitors of Alpha-amylase Activity. Braz. *J. Pharmacog.*, 16(1), 1-5 (2006).

23. Taleb A., Petit C. and Pileni M.P., Synthesis of Highly Monodisperse Silver Nanoparticles from AOT Reverse Micelles: A Way to 2D and 3D Self-Organization. *Journal of Physical Chemistry B*, 102(12), 2214-2220 (1998).

24. Noginov M.A., Zhu G., Bahoura M., Adegoke J., Small C., Ritzo B.A., Drachev V.P., and Shalaev V. M., Enhancement of Surface Plasmons in an Ag Aggregate by Optical gain in a Dielectric Medium. *Optics Letters*, 31(20), 3022-3024 (2006).

25. Link S. and El-Sayed M. A., Optical Properties and Ultrafast Dynamics of Metallic Nanocrystals. *Annual Review of Physical Chem*istry, 54(1), 331-366 (2003).

26. Kreibig U. and Vollmer M., Optical Properties of Metal Clusters. Vol. 25, Springer, Berlin (1995).

27. Nath S.S., Chakdar D. and Gope G., Synthesis of CdS and ZnS Quantum Dots and their Applications in Electronics. *Nanotrends-A journal of nanotechnology and its application*, 2(3), 20-28 (2007).

28. Mahmudin L., Suharyadi E., Utomo A.B.S, Abraha K., Optical Properties of Silver Nanoparticles for Surface Plasmon Resonance (SPR)-Based Biosensor Applications. *Journal of Modern Physics*, 6(8), 1071-1076 (2015).

29. Nideesh A., Jacob A., Krishnakumar S., Nanda A. and Dattaray D., Characterization of Chemical Mediated Synthesis of Silver Nanoparticles (AgNPs) and their Antibacterial Efficacy against Selected Bacterial Pathogens. *Der Pharmacia Lettre*. 8(8), 380-387 (2016).

30. Dhanalakshmi T. and Rajendran S., Synthesis of Silver Nanoparticles using Tridax Procumbens and its Antimicrobial Activity. *Arch. Appl. Sci. Res*., 4(3), 1289-1293 (2012).

31. Nath S. S., Chakdar D., Gope G. and Avasthi D., Effect of 100 Mev Nickel Ions on Silica Coated ZnS Quantum Dots. *Journal of Nanoelectronics and Optoelectronics*, 3(2), 180-183, (2008).

32. El-Deeb, N.M., El-Sherbiny, I.M., El-Aassara, M.R. and Hafez, E.E., Novel Trend in Colon Cancer Therapy using Silver Nanoparticles Synthesized by Honey Bee. *J. Nanomed. Nanotechnol.*, 6(2), 265-270, 2157-7439 (2015).

33. Ni, X.L. , Chen, L. X. , Zhang, H., Yang, B. , Xu, S. Wu, M., Liu, J. , Yang, L.L. , Chen, Y. , Fu, S.Z. and Wu, J.B., In vitro and In vivo Antitumor Effect of Gefitinib Nanoparticles on Human Lung Cancer, *Drug Delivery*, 24(1), 1501–151, (2017).

34. Sriram, M.I., Barath, S., Kanth, M., Kalishwaralal, K.. and Gurunathan, S. Antitumor Activity of Silver Nanoparticles in Dalton's Lymphoma Ascites Tumor Model. *Int. J. Nanomed*., 5, 753-762 (2010).

35. Abdel-Fattah, W.I., and Ali, G.W., On the Anti-Cancer Activities of Silver Nanoparticles. *J. Appl. Biotechnol. Bioeng*., 5(1), 43–46 (2018).

36. Kuppusamy, P., Ichwan, S.J., Al-Zikri, P.N., Suriyah, W.H. and Soundharrajan, I., In Vitro Anticancer Activity of Au, Ag Nanoparticles Synthesized Using *Commelina nudiflora L.* Aqueous Extract against HCT-116 Colon Cancer Cells. *Biol. Trace. Elem. Res*., 173(2), 297-305 (2016).

37. Zhang, X.F., Liu, Z.G., Shen, W. and Gurunathan, S., Review Silver Nanoparticles: Synthesis, Characterization, Properties, Applications, and Therapeutic Approaches, *Int. J. Mol. Sci*., 17(9), 1534 (2016).

38. Feng, Q.L., Wu, J., Chen, G.Q., Cui, F.Z., Kim, T.N. and Kim, J.O., A mechanistic Study of the Antibacterial Effect of Silver Ions on *Escherichia coli* and *Staphylococcus aureus*. *J. Biomed. Mater. Res*., 52(4), 662-668 (2000).

39. Sondi, S.SB. and Salopek-Sondi, B., Silver Nanoparticles as Antimicrobial Agent: A case Study on E. coli As A model for Gram-negative Bacteria.. *J. Colloid Interface Sci*., 275(1), 177-82 (2004).

40. Khandelwal, N., Kaur, G., Chaubey, K.K., Singh, P., Sharma, S., Tiwari, A., Singh, S.V. and Kumar, N., Silver Nanoparticles Impair Peste des petits ruminants Virus Replication. *Virus Res*., 190, 1–7 (2014).

41. Singh, H., Du, J. Priyanka Singh, P. and Yi, T.H., Role of Green Silver Nanoparticles Synthesized from *Symphytum officinale* leaf Extract in Protection Against UVB‐induced Photoaging. *J. Nanostruct. Chem*., 8, 359– 368 (2018).

42. Kaul, P.N., Kulkarni, S.K., Weinheimer, A.J., Schmitz, F.J. and Karns, T.K.B., Pharmacologically Active Substances from the Sea. III. Various Cardiovascular Activities Found in the Extract of Marine Organisms. *Lloydia*., 40, 253-259 (1977).

43. Arumugam, Dr.P., Khansahib, I. and Suriyanaarayanan, S., Green Synthesis of Nano-Particles and its Application in Treatment of Rheumatoid Arthritis. *Int. J. Comput. Geom. Appl*., 2(2), 450-457, (2013).

44. Venugopal, V., Marine Products for Healthcare: Functional and Bioactive Nutraceutical Compounds from the Ocean, CRC Press Taylor and Francis Group, 527, (2009).

45. Vijayaraj, R., Kumar, G. D., and Kumaran, N. S. In vitro anti-inflammatory activity of silver nanoparticle synthesized *Avicennia marina* (Forssk.) Vierh: A green synthetic approach. *Int. J. Green Pharm*., 12(3), 528-536 (2018).

46. Prabhu, D., Chinnasamy, A. and Gajendran, B., Synthesis and Characterization of Silver Nanoparticles using Crystal Compound of Sodium Para-hydroxybenzoate Tetrahydrate Isolated from *Vitex negundo*. L leaves and its Apoptotic Effect on Human Colon Cancer Cell Lines. *Eur. J. Med. Chem*., 84, 90−99 (2014).

47. Balan, K. , Qing, W. , Wang, Y., Liu, X., Palvannan, T., Wang, Y., Maa F. and Zhanga, Y., Antidiabetic Activity of Silver Nanoparticles from Green Synthesis using *Lonicera Japonica* Leaf Extract, *J. Chem. Soc.*, 6(46), 40162–40168, (2016).

48. Alkaladi, A., Abdelazim, A.M. and Afifi, M., Antidiabetic Activity of Zinc Oxide and Silver Nanoparticles on Streptozotocin-Induced Diabetic Rats. *Int. J. Mol. Sci.*, 15(2), 2015-2023 (2014).